Reprinted with permission Journal of Acoustical Society of America, Copyright 2008, Acoustical Society of America

Structural acoustics model of the violin radiativity profile

George Bissinger
Physics Department, East Carolina University, Greenville, North Carolina 27858

(Received 14 July 2008; revised 6 December 2008; accepted 6 December 2008)

Violin radiativity profiles are dominated by the Helmholtz-like $A0$ cavity mode (~280 Hz), first corpus bending modes $B1^-$ and $B1^+$ (~500 Hz), and BH and bridge-filter peaks (~2.4 kHz and ~3.5 kHz, respectively), with falloff above ~4 kHz. The $B1$ modes—dependent on two low-lying free-plate modes—are proposed to excite $A0$ via coupling to $B1$-driven in-phase f-hole volume flows. VIOCADEAS data show that $A0$ radiativity increases primarily as $A0$-$B1^-$ frequency *difference* decreases, consistent with Meinel's 1937 experiment for too-thick/too-thin plate thicknesses, plus sound post removal and violin octet baritone results. The vibration→acoustic energy filter, F_{RAD}, computed from shape-material-independent radiation and total damping, peaks at the critical frequency f_{crit}, estimated from a free-plate mode by analogy to flat-plate bending. Experimentally, f_{crit} decreased as this plate mode (and $B1^+$) frequency increased. Simulations show that increasing plate thicknesses lowers f_{crit}, reduces F_{RAD}, and moves the spectral balance toward lower frequencies. Incorporating string→corpus filters (including bridge versus bridge-island impedances) provides a model for overall violin radiativity. This model—with $B1$ and $A0$-$B1$ couplings, and f_{crit} (computed from a free-plate mode important to $B1$) strongly affecting the lowest and highest parts of the radiativity profile—substantiates prior empirical $B1$—sound quality linkages. © *2008 Acoustical Society of America.* [DOI: 10.1121/1.3006957]

PACS number(s): 43.75.De, 43.40.At [NHF] Pages: 4013–4023

I. INTRODUCTION

"The violin family presents many unsolvable problems; its shape and the peculiarities of its materials were certainly not selected with regard to convenience in analysis. This, however, only emphasizes the need for understanding the simplicities that do exist and may condone a certain amount of oversimplification." (Schelleng[1])

After two centuries of scientific work, Weinreich in 1992 distilled the continuing interest in the violin into "The New Secret of Stradivarius"[2] (edited form), viz., "… if we hand any experienced player a violin and ask that it be classified into one of three categories [student, decent professional, fine solo]… the judgment would not take more than about 30 s. … But the tantalizing fact is that *no such specification which successfully defines even coarse divisions in instrument quality is known*." (Weinreich's italics). Even a much-expanded set of descriptive parameters made possible by utilizing some of the latest technologies for simultaneous vibration and radiation measurements on 17 bad-good-excellent quality-rated violins, including three-dimensional (3D) modal analyses of three exemplary old-Italian violins, showed little in the way of quantitative "robust" differences between excellent and bad violins, with one notable exception.[3]

Since a great violinist can make a bad violin sound good, while a bad violinist cannot make a great violin sound good (see Saunders' remarks about Jascha Heifetz and the "standard-of-badness" violin[4]), the violinist's ability to manipulate the *relative* harmonic strengths in the driving force, which does not in any way affect the violin itself, clearly can compensate for perceived acoustic deficiencies. Consider also that violinists preferring a certain type of sound might reasonably be expected to pick just those violins that best give them that sound. Two conclusions—one obvious, and one more subtle—can be drawn: (1) the major determiner of violin sound quality is the violinist, not the violin; (2) even a "bad" violin somehow contains the essence of good-violin sound, needing only the proper driving force at the bridge to elicit its capabilities. Considering just the implications of earlier research by Meinel,[5] Saunders, and Dünnwald,[6] this is hardly a new conclusion.

However, when violins of the same shape, materials, and construction show similar low-lying "signature" modes and similar overall band-average mobility and radiativity profiles,[3] we might logically deduce that properly setup violins *are* pretty much the "same." (A physics-based argument based on building a solid model in a finite element program will reach a similar conclusion.) This seemingly unhappy inference recommends a different potentially positive change in perspective. Without an evanescent "secret" to pursue, an alternate approach employing relatively few normal modes—the "atoms" of vibration—rather than a conglomerated response of all the modes at particular frequencies, when combined with measured radiation and damping properties, offers a powerful tool that readily marries materials and responses.

Furthermore, if we allow that the relative *proportions* of certain behaviors can cause a much more strongly differentiated *psychoacoustic* response than underlying measurable mechanical-acoustic changes would seem to warrant (see Ref. 5 for such comments), a viable basis for reliable quality differentiation by the violinist—but not the scientist—becomes quite feasible. (Akin to how adding a very little salt—relative to the overall mass—can greatly change the perceived taste of a steak.)

Adopting this "sameness" conjecture and relying on the zero-mass-loading excitation-response, normal-mode and materials database that includes 3D modal analyses[3]—hereinafter labeled by the acronym VIOCADEAS (VIOlin Computer Aided Design Engineering Analysis System)[7]—we search for plausible structural acoustics mechanisms to produce similar, but "different," radiativity profiles that modulate driving-force harmonics to create violin sound. While this analysis has elements of speculation, oversimplification, and, given its subject, controversy, it should be viewed rather as an attempt, in the spirit of Schelleng, to make "systems-level" sense of the overall shape of the violin radiativity profile.

II. EXPERIMENTAL SYSTEMATICS

Radiativity $R(\omega)$ is the complex ratio of pressure/force; all VIOCADEAS far-field pressures (and surface velocities) were normalized to the driving-force applied at the violin bridge G-corner, then mean square averaged over 266 microphone measurements around a sphere in an anechoic chamber[3] to create a rms radiativity $\langle R\rangle$. $\langle R\rangle$ was then frequency band averaged to create a radiativity "profile," a simplified "parameter" at the end of the energy chain closely allied to what the violinist hears when holding and playing the violin.

The other crucial parameter was mobility $Y(\omega)$, the complex ratio of surface velocity/force, mean square averaged over the corpus (top+ribs+back) to create rms corpus mobility $\langle Y_{\text{corpus}}\rangle$. The new 3D mobility measurements offered important insights into extensional ["in plane" (IP)] motions as well as the flexural ["out of plane" (OP)], especially so in the region around the bridge feet labeled the "bridge island."[3] (Coordinate system origin on the top plate between bridge feet: Y-axis perpendicular to the violin "plane," X-axis across, and Z-axis along the violin.)

A. Mobility-radiativity systematics

VIOCADEAS band-averaged profile results for $\langle R\rangle$ (17 violins) and $\langle Y_{\text{corpus}}\rangle$ (14 violins, surface-normal direction) are shown in Fig. 1 [standard deviation (s.d.), error bars denote *intraband* variations only]. Earlier analysis, judging only the magnitude of radiativity across the whole 4 kHz span, concluded that "excellent" (all old-Italian) violins had no advantage over bad violins overall. Quality-related differences in radiativity profiles were characterized simply by noting that excellent violins had somewhat flatter (without ever being flat), less compressed along the frequency axis, less-peaky overall profiles, with higher values at the frequency extremes.[3] Below 4 kHz only one significant difference between bad and excellent violins was observed: $A0$, the only resonance in the lowest octave, was significantly stronger for excellent violins than bad, with "good" violins having intermediate values.

In 1946, Saunders, the pre-eminent American violin researcher of his time, summarized decades of research on the violin (including close interactions with violinists such as Jascha Heifetz), by noting that eminent violinists wanted two qualities in a violin: "first, great power, and second, an even distribution of strength among all ranges of frequency, *the lowest octave being of special importance* [my italics]."[4] VIOCADEAS data show a clear dependence of the so-called "warm, full" quality criterion on $\langle R_{A0}\rangle$. Clearly, Saunders' observation is still right to the mark.

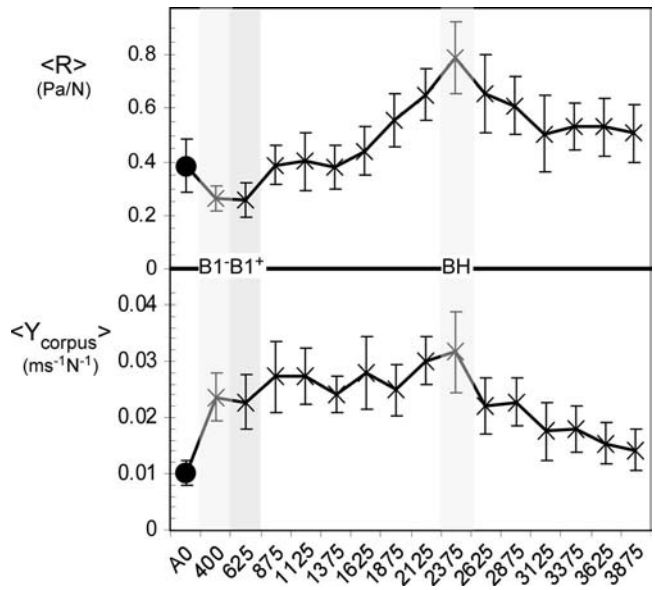

FIG. 1. (Top) 17-violin radiativity $\langle R\rangle$ and (bottom) 14-violin corpus mobility $\langle Y_{\text{corpus}}\rangle$ vs band-center frequency ($A0$, ●). BH peak near 2.4 kHz. (s.d. error bars reflect intraband variations only.)

We commence with a brief description of the signature modes common to all violins tested (and to a complete violin octet[8]). These are of particular importance to this discussion since they determine the acoustic output for harmonics in the crucial open string region 196–660 Hz. Signature modes fall into two major classes: (1) *cavity modes*: $A0$-Helmholtz-like, $f_{A0}\approx 280$ Hz, characterized as dual mass plugs oscillating in phase in the f-holes under the influence of the cavity "spring," always the lowest frequency mode in the violin and always a strong radiator, and $A1$—the first longitudinal mode, sometimes an important radiator (via induced surface vibrations) with $f_{A1}\approx 1.7x f_{A0}$, coupled to $A0$ and strongly affecting its volume dependence;[9] (2) *corpus modes*: CBR—the lowest corpus mode near 400 Hz, weakly radiating, with shear-like (along X) relative motion between the top and back plates, and out-of-phase f-hole volume flows, and, most importantly, the first corpus bending modes $B1^-$ and $B1^+$ near 500 Hz, both strong radiators with in-phase f-hole volume flows and strong radiation from the f-holes. (All f-hole volume flow remarks are based on recent "patch" near-field acoustical holography pNAH results from Ref. 10 where a high-spatial-density near-field microphone array was scanned over a rectangular patch above the f-holes, with pressures postprocessed to estimate volume flows from just the f-holes).

Although band averages were normally taken over 250 Hz intervals, the two lowest bands were modified to isolate $A0$ near 280 Hz with an average over the peak ± 10 Hz. The 400 Hz band, averaged from 300–499 Hz, included the CBR, $A1$, and $B1^-$ modes. The next band

(500–749 Hz) centered at 625 Hz was dominated by $B1^+$, near 550 Hz. Thus $A0$, $B1^-$, and $B1^+$ dominate the radiativity in these three bands, as notated in Fig. 1.

$\langle R \rangle$ starts high at $A0$ (its very low $\langle Y_{\text{corpus}} \rangle$ clearly distinguishes it from corpus modes), drops down, and then rises again as the combined effect of increasing $\langle Y_{\text{corpus}} \rangle$ and radiation efficiency R_{eff} makes $\langle R \rangle$ grow faster than $\langle Y_{\text{corpus}} \rangle$. Above the BH peak near 2.4 kHz, $\langle R \rangle$ falls off more slowly than $\langle Y_{\text{corpus}} \rangle$ because R_{eff} increases up to the average effective critical frequency $f_{\text{crit}} \approx 3.9$ kHz.[3]

Overall $\langle Y_{\text{corpus}} \rangle$ grows more slowly to its maximum at the BH peak but declines more rapidly above. Although clearly depending on the bridge, this peak has a weak dependence on the bridge top rocking mode frequency f_{rock};[11] experiments by Durup and Jansson have shown that cutting the f-holes is crucial to the appearance of this peak.[12] The $\langle R \rangle / \langle Y_{\text{corpus}} \rangle$ ratio used to estimate f_{crit} showed a relatively smooth behavior well described by a linear trendline.[3] The BH band, except for its magnitude, did not display any unusual attributes, such as unusually large/small R_{eff} or total damping relative to bands below-above. The BH peak in $\langle R \rangle$ thus appears to arise from a mobility peak. Above the BH peak $\langle Y_{\text{corpus}} \rangle$ declines somewhat more rapidly than it grew.

III. RADIATIVITY PROFILE ANALYSIS

To understand the major components of a violin's radiativity profile, it is necessary to (1) establish an $A0$ excitation mechanism at the low-frequency end, aided by pNAH characterizations of f-hole volume flows, (2) understand $B1$ mode dependence on the plate modes 2 and 5, (3) examine extensional-flexural behaviors in the bridge-island region, (4) incorporate bridge-filter effects, (5) treat the plates as flat (successfully used in scaling the violin octet[1,8]), and then (6) exploit R_{eff} and f_{crit} systematics. This analysis starts at the low-frequency end and works up.

A. *A*0-*B*1 coupling

Certainly the most important cavity mode in the violin, strong $A0$ was singled out by Dünnwald as one of five good-violin quality attributes in his 700-violin survey,[6] a conclusion strongly supported in the VIOCADEAS excellent to bad radiativity comparison.[3] Since $A0$ is the only strong radiator in the violin's lowest octave, how exactly do corpus vibrations excite this cavity mode? Cremer addressed this problem by creating an "island" model, believed reliable for the first three or four response peaks (the signature mode region, thereby implying that only corpus modes near $A0$ in frequency were plausible excitation candidates), stating that the cause was "…excitation of the air oscillating in f-holes by the lever mechanism of the bridge; the front and back compress and rarefy the cavity equally and in phase."[13] This model thus assumes direct mechanical excitation where the top plate region in contact with the sound post was coupled via the rigid sound post to the back plate, all moving in phase, with the bass bar bridge foot moving antiphase.

VIOCADEAS results, however, provide a much different view of corpus motion: animations show bridge rigid-body-rocking motion pivoting about the relatively fixed soundpost foot for $A0$ (and $B1$), with maximum amplitude on the bass bar—not sound post—side. CBR, the lowest corpus mode lying between $A0$ and $B1$, does show equal amplitude, antiphase motion for the bridge feet. At frequencies above $B1$ (>0.7 kHz), the motion of the two feet was again approximately equal.[11] Moreover computed corpus-motion-driven volume flows at f_{A0} were almost a factor of 10 smaller than measured $A0$ f-hole volume flows.[10] Obviously an alternative $A0$ excitation mechanism was needed.

It is axiomatic in vibrations that to excite a mode strongly, it is necessary to drive its motion at—or near—an antinode in a way that does not modify its properties significantly, at a frequency close to the resonant frequency for that mode. The fact that $A0$ and the close-by low-lying corpus modes have the largest total damping is obviously advantageous in spreading the response. $A0$ has been characterized experimentally as Helmholtz-like, i.e., having oscillating in-phase volume flows (mass-plug motions, influenced by the cavity volume spring), independent of compliant violin cavity walls[14] or the coupling to $A1$.[9] Such in-phase f-hole volume flows thus define $A0$'s antinodes.

General physical arguments offer support for Cremer's neglect of high-frequency modes as plausible candidates for exciting $A0$: (1) "direct" f-hole volume flows driven by net-volume-change modes are important only where the internal pressure is approximately constant over the cavity, a condition satisfied only by modes below about 0.7 kHz;[10] (2) except for the BH peak, mobility drops with increasing frequency above about 1 kHz (see Fig. 1) and the receptance (displacement/force) falls off as mobility/frequency, hence net-volume changes will drop faster than $1/f$, possibly as fast as $1/f^2$ above 2.4 kHz; (3) since mode shapes increase in complexity as frequency increases, with decreasing nodal line separation and thus smaller possible displacements, the effect again is to decrease net-volume change. All these factors taken together argue strongly against higher frequency modes contributing significantly to $A0$ excitation.

To excite $A0$, *low-lying* corpus modes then should have strong in-phase f-hole volume flows close to $A0$ in frequency. In order of increasing mode frequency, it is possible to eliminate both $A1$, which does not have in-phase f-hole volume flows, rather each f-hole shows acoustic "short" volume flows, and CBR, which has antiphase f-hole volume flows and small volume changes. Below 0.7 kHz, this leaves only the next-higher corpus modes, $B1^-$ and $B1^+$, as likely candidates to excite $A0$ since they are (a) close by, (b) always strongly excited, and (c) radiate ~50% from the f-holes via significant in-phase f-hole volume flows.

$B1$ f-hole volume flows driving $A0$ imply relative $A0$-$B1$ f-hole volume flows have a phase lag and $\langle R_{A0} \rangle$ should increase as the frequency difference Δf between $A0$ and the $B1$ modes decreases. Since cavity mode excitation must in some way come via the corpus, a phase-lag would be expected in any case. Animations of pNAH and modal analysis data with f-hole air and plate motion in proper phase show that $A0$ clearly lags $B1$ by ~90°. (This phase lag can be seen less clearly in the volume velocity holograms, Fig. 4 in Ref. 10).

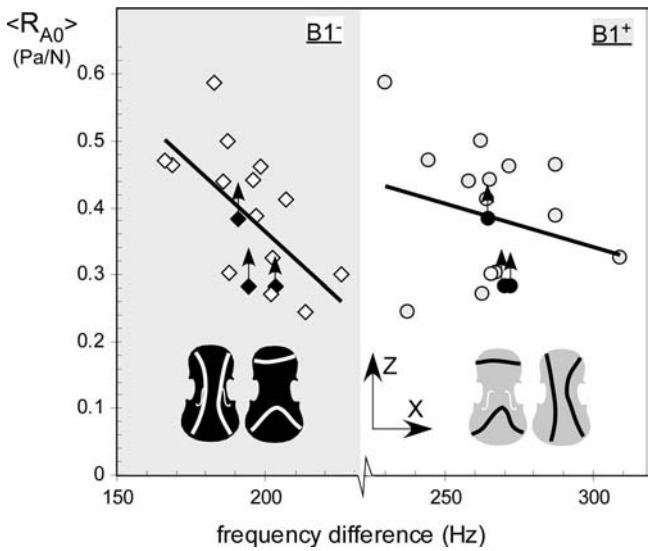

FIG. 2. $\langle R_{A0}\rangle$ vs $A0$-$B1^-$ and $A0$-$B1^+$ Δf (empirical trendlines). The filled points have strong substructure coupling "dimpling" the $A0$ peak; the arrows indicate approximate corrections (not used for trendline fit). Nominal top-back $B1$ nodal patterns shown along with coordinate frame axes.

The Δf argument is substantially more powerful. The proposed $A0$-$B1$ coupling mechanism implies a stronger correlation with $B1^-$ than $B1^+$ since it is closer in frequency. A scatter plot of VIOCADEAS $\langle R_{A0}\rangle$ vs Δf data is shown in Fig. 2. The falloff of $\langle R_{A0}\rangle$ with increasing Δf appears clear for $B1^-$ but only "suggestive" for $B1^+$. Three violins had strong substructure coupling, dimpling the $A0$ peak (filled points in Fig. 2) and thus reducing $\langle R_{A0}\rangle$. Without this dimple $\langle R_{A0}\rangle$ would increase; empirical corrections shown in Fig. 2 indicate approximate magnitudes for the "dimple" effect. However, empirical linear trendline equations—$\langle R_{A0}\rangle = -0.0041\Delta f + 1.18$ (Pa/N) ($r=0.62$) for $B1^-$ and $\langle R_{A0}\rangle = -0.0013\Delta f + 0.74$ (Pa/N) ($r=0.25$) for $B1^+$ used uncorrected data.

VIOCADEAS data thus provide support for $A0$-$B1$ coupling, with $B1^-$ more important than $B1^+$ in exciting $A0$ (cf. Fig. 2, Ref. 3 where transposition of $B1^-$, $B1^+$ relative mobility magnitudes for bad-excellent violins is mirrored also by observed $\langle R_{A0}\rangle$). The hypothesis that $\langle R_{A0}\rangle$ increases as $A0$-$B1$ Δf decreases (and vice versa) can now be put to the test against appropriate earlier experiments, some dating back to 1937.

1. A0, plate thickness, and B1

In 1937, Meinel investigated the effect of reducing plate thicknesses from too-thick to normal to too-thin on violin radiation curves.[15] A graphic based on his Fig. 3 for just the $A0$-$B1$ region is shown in Fig. 3. Prominent peaks identified as the $B1$ corpus mode peaks dropped almost 200 Hz (graphical estimate) as plates were successively thinned, while the lowest peak, $A0$, remained near 270 Hz (± 15 Hz). VIOCADEAS data show $A0$ often coupling with various substructures like the neck-fingerboard and tailpiece; some such behavior was seen in these plots. Meinel's results show $B1$ radiation changed relatively little as $A0$-$B1$ Δf dropped by nearly a factor of 2; $A0$ radiation however grew approximately 8x. The enormous $B1$ variation extended far beyond our linear trendline region, hence a new power-law trendline for conglomerated $B1$ data, $\langle R_{A0}\rangle = 1.65x10^4 \Delta f^{-2.4}$ (Pa/N), was used to estimate Meinel's too-thick:too-thin pressure ratio as 6:1, consistent with experiment.

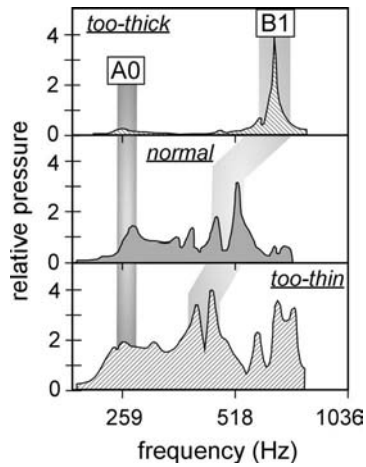

FIG. 3. Relative pressure readings for violin with too-thick, normal, and too-thin plates (after Meinel, Ref. 15, Fig. 3). $A0$, $B1$ labeled, and frequency-shift trends highlighted.

2. A0 and the sound post

Meinel also investigated the effect of the sound post on the acoustic output of the violin, shifting from tight-post to loose-post to no-post. Sound post removal produced two major effects: (1) $A0$ frequency dropped from $\sim$270 to $\sim$240 Hz due to the loss of cavity wall stiffening provided by the sound post, and (2) $A0$ acoustic output fell off to $\sim 1/3$ of the (normal) loose-post value.

Similar effects were observed in a 1995 sound post removal modal-acoustic analysis experiment: (1) $A0$ dropped from 279 to 245 Hz, (2) $A0$ acoustic output dropped significantly, (3) $\langle Y_{\text{corpus}}\rangle$ at $B1^-$ ($f \approx 500$ Hz) decreased substantially with sound post removal, at $B1^+$ ($f \approx 550$ Hz) $\langle Y_{\text{corpus}}\rangle$ showed an equally significant increase.[16] Room-average acoustic analysis, however, showed decreased acoustic output for both modes; boundary element method calculations indicated that for the peak associated with $B1^+$, falloff was due to a large R_{eff} decrease. Since $A0$-$B1^-$ Δf increased and the strength of $B1^-$, the most important mode in this coupling, decreased, the observed $A0$ falloff was consistent with $A0$-$B1$ coupling. Increased $B1^+$ excitation did not compensate for these two factors. (A cautionary note: although mode frequencies were seemingly little affected, the no-soundpost mode closest in frequency to $B1^-$ had a significantly different mode shape, implying that f-hole volume flows could be altered.)

The modal analysis data added significant insight into what happens at the bridge feet on sound post removal: (1) at the 245 Hz $A0$ frequency, the bridge feet moved significantly more and in phase, (2) both feet moved in phase at $\sim$500 Hz and antiphase at $\sim$550 Hz, with similar amplitudes for each foot, and (3) the $\sim$500 Hz mode had less amplitude overall, while the $\sim$550 Hz mode had more.

3. A0-B1 coupling and the violin octet

Modal and acoustic analysis of a complete violin octet generally supported Schelleng's flat-plate scaling procedure in placing $B1$ in the proper relationship to open string tunings and relative to $A0$, with one notable exception, the baritone's $B1$ frequencies.[8] These were by far the highest relative to desired placement across the entire octet, three semitones higher than desired. Baritone $A0$ radiation was also surprisingly weak compared to all other instruments in this set (see Fig. 1, in Ref. 8). $A0$-$B1$ coupling readily predicts significantly reduced $A0$ radiation for baritone $B1$ considerably above the scaling goal.

B. The B1 modes

Empirical relationships discovered recently between the top and back plate bending mode 2 and 5 frequencies and the average $B1$ frequency and frequency spread Δf, with strikingly similar nodal patterns,[17] indicate that these plate modes are effectively subsumed into the low-lying first corpus bending modes $B1^-$ and $B1^+$. A *heuristic* flat-plate dynamic stiffness model incorporating rib bending stiffness supports these observed experimental trends.[17] (This bending mode analogy relates also to f_{crit}, discussed later.)

C. Moving up the R_{eff} curve

The VIOCADEAS radiativity profile rises above the $B1$ peaks, reaching a maximum near 2.4 kHz, and then falling off slowly.

1. The bump near 1.2 kHz

This is a difficult region because it varies between quality classes (the so-called "nasal" region) and has a number of different possible contributors: (1) maximum in the bridge:bridge-island Y-direction impedance ratio,[3] (2) presence of nominal f_{ring} value for this quasicylindrical form,[7] (3) very significant f-hole radiative contributions[10] (4) excellent R_{eff} above average, bad below, (5) excellent $\langle Y_{\mathrm{corpus}}\rangle$ below average, bad above, (6) near maximum modal density.[7] All factors might contribute or just a few, hence no clear understanding of this complex region has emerged.

2. The BH peak near 2.4 kHz

The BH peak at 2.4 kHz in Fig. 1 appears at each step in the violin's energy chain—driving point at the bridge corner, averaged-over-bridge, bridge feet (corpus immediately adjacent to bridge feet), averaged-over-corpus, and in the averaged radiativity.[11] It does not, however, show up in unusual R_{eff} or ζ_{tot} values, from which we infer that it arises from vibrational enhancement effects originating in the bridge-corpus coupling.[3]

The 3D corpus modal analyses of three violins has allowed us to discern important new violin vibrational behaviors in the bridge-island region between the f-holes:[3] (1) only the X-component of mobility displayed a peak near 2.4 kHz (Fig. 2 shows the X-Z axes), (2) the Y-component peaks near 1 kHz, decreasing monotonically above, (3) the X-component ranged from $\sim 30\%-70\%$ of the Y-component, and (4) the Z-component was weakest. The fact that the sound post, bass bar, and f-holes are concentrated in the very region where string energy enters the corpus through the bridge feet makes this island region rich in the very boundaries-discontinuities needed to transform extensional into flexural motion. Another possibility gleaned from a combination of one-dimensional bridge mobility results with 3D corpus results was a narrow minimum in the bridge/bridge-island impedance ratio at 2.4 kHz for both X and Y components.[3] A maximum in X-extensional motion (transformed somehow into flexural motion) coinciding with an impedance matching effect suggests plausible mechanisms for the relative prominence of the BH peak in the mobility spectra.

Above 2.4 kHz, the effect of the bridge is conspicuous. Small waist trims to tune this substructure (clamped feet, adjust f_{rock}) have substantial effects on the radiativity profile (and perceived quality).[11] Significant progress has been made of late in modeling the bridge filter,[18,19] although additional effort will be necessary to understand the complexities of bridge-corpus coupling when significant extensional foot motions are involved.

3. SMI parametrization

For a shape so complex and materials so variable, any attempt to interpret a violin's general high-frequency radiativity must rely on shape-material-independent (SMI) structural acoustics parameters (but violin mass and "size" are still relevant). The SMI parameters chosen are (1) R_{eff}, (2) f_{crit}, (3) total damping ζ_{tot} (% of critical) extracted from mobility peak fits, (4) radiation damping ζ_{rad} (% of critical, computed with R_{eff}, f and mass), and (5) $F_{\mathrm{RAD}}=\zeta_{\mathrm{rad}}/\zeta_{\mathrm{tot}}$, the fraction of vibrational energy radiated. Structural acoustics systematics for these parameters provide a "stylized" representation versus frequency:[20] (a) $R_{\mathrm{eff}}\propto f^2(f\leqslant f_{\mathrm{crit}})$, $R_{\mathrm{eff}}=1(f>f_{\mathrm{crit}})$,[3] (b) $\zeta_{\mathrm{tot}}\propto f^{-1/2}$,[21] a violin rule of thumb [note: isolated top and back plate substructures had $\zeta_{\mathrm{tot}}\approx$ const (Ref. 20)]; (c) $\zeta_{\mathrm{rad}}\propto f(f\leqslant f_{\mathrm{crit}})$; $\zeta_{\mathrm{rad}}\propto f^{-1}(f>f_{\mathrm{crit}})$. Radiation damping for $A0$ is expected to be about $0.5\zeta_{\mathrm{tot}}$,[13] hence $F_{\mathrm{RAD}}\approx 0.5$ for $A0$, for all violins.

A F_{RAD} "leaky bucket" characterization of energy loss incorporates ζ_{rad}, ζ_{int} internal (heat)—small compared to any violinist's support fixture damping—and ζ_{fix} support fixture losses that sum to ζ_{tot}. VIOCADEAS measurements effectively eliminated support fixture losses, so $\zeta_{\mathrm{fix}}\approx 0$. Computing $\zeta_{\mathrm{int}}\approx\zeta_{\mathrm{tot}}-\zeta_{\mathrm{rad}}$ showed it to be hardly different between excellent and bad violins, although quite significant at low frequencies where ζ_{rad} is small.[3] Thus at low frequencies, $\zeta_{\mathrm{rad}}\ll\zeta_{\mathrm{tot}}$, $\zeta_{\mathrm{tot}}\approx\zeta_{\mathrm{int}}\propto f^{-1/2}$. Presuming $\zeta_{\mathrm{int}}\approx Cf^{-1/2}$ across our frequency range guarantees that the ζ_{tot} frequency dependence is maintained at lower frequencies while maintaining a consistent simple falloff behavior up to 8 kHz.

These assumptions provide quite reasonable agreement with the conglomerated 14-violin data for ζ_{tot} (%critical), ζ_{rad} (%critical), and F_{RAD} as shown in Fig. 4 [effective $f_{\mathrm{crit}}\approx 3.9$ kHz (Ref. 3)]. Only the internal damping equation coefficient C was varied to optimize agreement between ex-

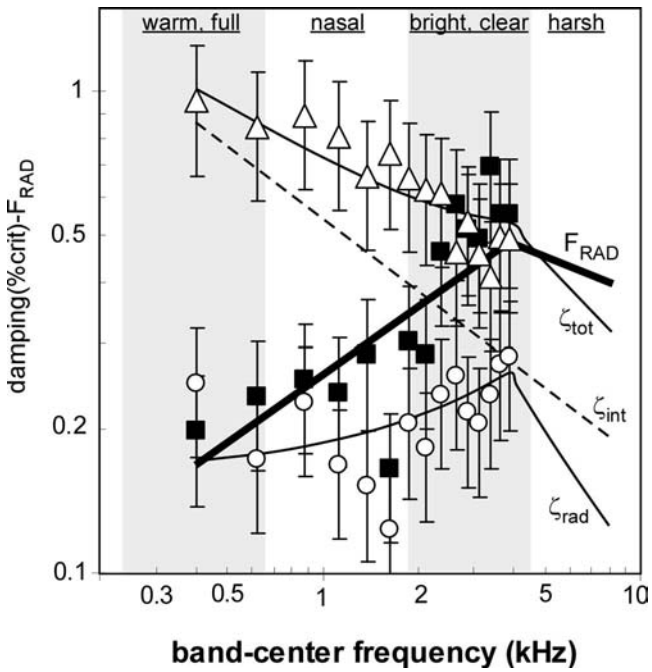

FIG. 4. (log) 14-violin corpus ζ_{tot} (△) and ζ_{rad} (○), and F_{RAD} (■) vs (log) band-center frequency ($f_{crit} \approx 3.9$ kHz) compared with stylized representations for each. (ζ_{rad}, $\zeta_{tot} \pm 30\%$ s.d. error bars represent average intraband variations; ζ_{int} represented by dashed line common to all violins.)

perimental and computed ζ_{tot}. Also in Fig. 4 are qualitative terms related to relative prominence of certain frequency bands (after Dünnwald[6]).

4. Perceived loudness

The fact that excellent and bad violins overall showed similar averaged-over-sphere $\langle R \rangle$ seems on its face inconsistent with Saunders' remark about "great" violins being loud. There are, however, two straightforward ways perceived loudness can be enhanced while still being consistent with VIOCADEAS results: (1) since violins radiate more strongly into the top hemisphere than the back, make violins radiate even more strongly by somehow changing the top plate flexural-extensional motion ratio, or possibly the arching (cf. Figs. 7 and 8 in Ref. 3); (2) emphasize regions where the ear is most sensitive—2–4 kHz—in the vibration-radiation conversion.

Pertinent to the second point, an experiment trimming the bridge waist in two ~2 mm steps (~0.02 g/step) dropped the bridge rocking frequency f_{rock} from 3.4 to 3.0 to 2.6 kHz, reduced maximum radiativity in the 2.5–4 kHz region by a factor of ~3, and made a good violin bad.[11] A perceptible but difficult-to-quantify slippage of the peak toward lower frequency was observed (see inset of Fig. 5). The fact that a poor bridge can make the sound of a very good violin quite bad—not by changing the violin's underlying normal modes, just their proportionate involvement in the overall vibrations—underscores the importance of the bridge filter on the overall radiativity profile in the ear's most sensitive range.

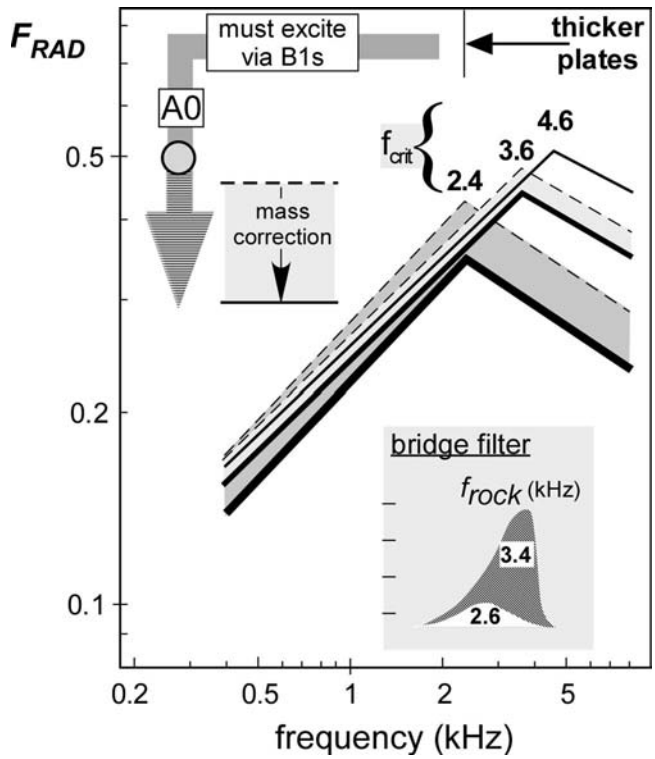

FIG. 5. (log) F_{RAD} vs (log) frequency for f_{crit}=2.4, 3.6, and 4.6 kHz (BH peak, old-Italian, and highest, respectively). *A*0 value fixed (but excitation via *B*1 crucial). Gray areas under each curve indicate schematic correction for increasing plate mass relative to 4.6 kHz curve. [Inset: effect of f_{rock}, 3.4–2.6 kHz, on (linear) radiativity, same frequency scale (after Fig. 10, Ref. 11).]

5. Critical frequency and F_{RAD}

A violin "equation" $I(\omega) \propto P^2(\omega) \propto F^2(\omega)\langle Y^2_{corpus}(\omega)\rangle R_{eff}$ provides a reasonable first approximation for quantifying sound intensity from the violin.[20] The first term on the rhs represents the driving-force energy input to the bridge, the second term represents the "gatekeeper" filter for bridge-corpus energy transfer, the third term represents the vibration-radiation energy conversion "egress" filter. Since the radiativity profile convolutes the second and third terms, F_{RAD}, which deals only with corpus energy loss via various damping mechanisms, was used to create in effect a "bridgeless" violin with only the "egress" filter.[22] The simple behavior of F_{RAD} as f_{crit} is varied provides important insights into the crucial role of f_{crit} in shaping the radiativity profile.

F_{RAD} simulations for varying f_{crit} (keeping $\zeta_{fix} \approx 0$) appropriated the ζ_{int} trendline from Fig. 4. The ζ_{rad} maximum was then moved to successive f_{crit} values, and the ζ_{rad} trendline equation adjusted accordingly. *A*0 F_{RAD} remained constant. Simulated F_{RAD} curves are shown in Fig. 5 for f_{crit}=2.4, 3.6, and 4.6 kHz, corresponding to the BH peak, two-old-Italian average, and highest measured f_{crit} value. Since f_{crit} changes would primarily be due to varying plate thickness *h* (using flat rectangular plate theory as a guide), $f_{crit} \propto 1/h \propto 1/\text{plate mass}$ (assuming a constant density-stiffness relationship[23]). Since $\zeta_{rad} \propto 1/\text{violin mass}$, and plate-mass is nominally 1/2 violin mass, a crude correction for increasing plate mass (relative to the 4.6 kHz curve) was computed and shown graphically as shaded areas underneath

the 2.4 and 3.6 kHz curves. The relative importance of the gatekeeper and egress filters can be gauged from the inset of Fig. 5 showing an abstracted representation of the effect of changing bridge f_{rock} from 3.4 to 2.6 kHz (after Fig. 10, Ref. 11).

Maximum corpus F_{RAD} always falls at f_{crit}. As f_{crit} decreases, peak F_{RAD} values also drop due to the increasing ζ_{int} contribution to ζ_{tot} and increasing plate mass/thickness. A fixed $A0$ $F_{RAD} \approx 0.5$ becomes relatively more important as f_{crit} decreases, especially when compared to F_{RAD} values above 3 kHz, signaling a shift in spectral balance toward lower frequencies for low f_{crit} values. An important caution: as $A0$ *excitation* relies on $A0$-$B1$ coupling this must be kept in mind when discussing the overall spectral balance shifts. Decreasing f_{rock} (fixed f_{crit}) also affects the spectral balance similarly. Entirely independent of how the corpus gains vibrational energy via the gatekeeper filter, it is always around f_{crit} where the violin most efficiently turns corpus vibrational energy into radiation. Even when the violin is held-played and violinist ζ_{fix} dominates ζ_{tot}, relatively unaffected normal-mode shapes[24] indicate that R_{eff} should remain close to free-free values, as should f_{crit}. F_{RAD} magnitudes, however, drop significantly.

6. Extended radiation plots

If old-Italian radiativity profiles somehow define the psychoacoustic first choice for "desired" sound, how can these be realized in practice? In 1990, Dünnwald, using electromagnetic excitation via a highly damped wire at a bridge corner, published radiation measurements up to 7 kHz on 700 violins with a single far-field microphone in an anechoic chamber.[6] Our radiativity results support many of his conclusions. The broad agreement between the overall profiles, from different data sets, is important because it confirms the generality of both results and suggests using both data sets in a general analysis exploring the connection between the top and back plates, which dominate the mass and surface area of the violin, and the violin radiativity profile.

Dünnwald's superposition plots are represented in Fig. 6 via their envelopes as "conglomerated" radiation profiles corresponding to "averaged" *10-old-Italian*, *10-master*, and *10-factory* subsets. These subsets present quite different profiles. Two important features emerge: (1) most prominently, the remarkable change in acoustic radiation above 2.5 kHz; the 10-master violins have a much extended frequency range compared to the 10-factory violins, while the 10-old-Italian envelope is intermediate; (2) less obvious, but equally important, a shift in average $B1$ frequency among these subsets. The 10-old-Italian $B1$ envelope region with two separated peaks near 500 Hz (almost certainly the first corpus bending modes $B1^-$ and $B1^+$) was also quite different from the other two, which appeared as a broad mush.

What more need be said about these instrument classes? Old Italian violins, from a relatively few now-legendary violin makers, are a revered class that, enjoying the very best care and maintenance and almost universally involving substantial repair work, have undergone considerable change to keep current with evolving performance requirements. Factory violins with machine-figured too-thick plates fall at the other end of the care-maintenance spectrum, with master violins somewhere in between. These become important distinctions in our analysis.

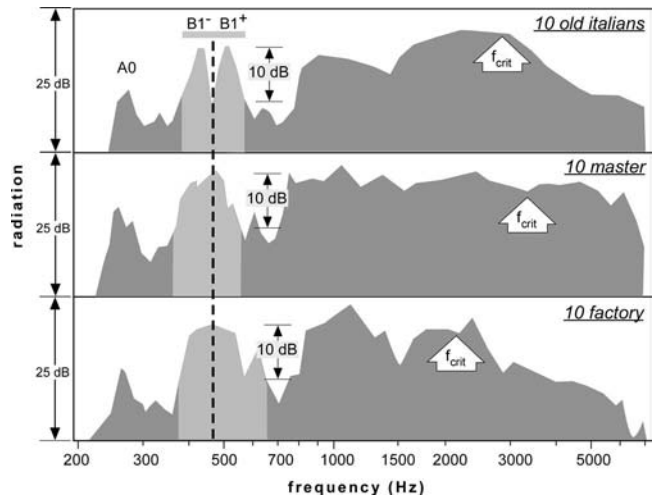

FIG. 6. 10-violin envelope curves after Dünnwald superposition plots (Ref. 6, Fig. 3). The vertical dashed line locates average B1 for 10-old-Italian envelope for reference to 10-master and 10-factory $B1$; the arrows denote plate-mode-5-based f_{crit} estimates for each envelope.

IV. CRITICAL FREQUENCY LINK

For centuries, the top and back plates were the only substructures with resonance frequencies determined prior to assembly, using tap tones (many use Chladni patterns now) to tune plates to "prescribed" frequencies prior to assembly. We conjecture that top and back plate bending modes 2 and 5—subsumed into the low-lying first corpus bending modes[17]—are key to understanding relationships between these radiativity profiles. This relationship—the crucial link between the violin f_{crit} and plate mode frequencies—is based on the fundamental physics underlying the critical frequency concept, the dispersive flexural wave velocity v_f catching up with the velocity of sound $c(\approx 344\ \mathrm{m/s})$.

A historical note germane to the Dünnwald 10-master violin envelope concerns the lack of agreement on what these prescribed frequencies should be. In 1885, Heron-Allen remarked that some makers were tuning the back lower than the top, which he emphatically stated was entirely wrong: "Nearly every author who has written on this subject has declared that *the back should be a tone lower* than the belly. It is useless (as many of them probably never actually *made* a fiddle) to persuade them that exactly the reverse is the case."[25] We might conjecture from this that master violins can have quite variable plate tunings. This variability was reflected in the VIOCADEAS database, where mode 5 top/back frequency ratios varied from 0.90 to 1.03, obviously not all in harmony with Heron-Allen's dictum.

On the other hand, factory (machine-figured) violins normally have too-thick plates and old-Italian violins presumably a relatively standardized tuning as suggested by the $B1$ mode placement separation in Fig. 6.

A. Plate mode: Critical frequency link

The 14-violin $f_{crit} \approx 3.9$ kHz was in good agreement with the along-grain 4.5–4.9 kHz values computed for violin-size flat rectangular spruce and maple wood plates by Cremer;[13] cross-grain f_{crit} values were one-two octaves higher. (Along- or cross- grain notation here relates to flexural wave motion relative to grain direction, which runs along the violin long axis.) This agreement suggests a plate $\rightarrow$violin f_{crit} linkage. Since little input energy is available at frequencies above 6–8 kHz from the nominal sawtooth bowing force (nth harmonic $\propto 1/n^2$), a high f_{crit}-low input energy combination implies along-grain flexural motions will predominate in violin sound; hence our discussion is limited to this case.

1. Additional simplifications

Some additional simplifications-assumptions to estimate f_{crit}: (1) the top and back plates, which dominate the radiating area of the violin, are the only important radiating surfaces, and the top plate is more important; (2) v_f is the same in free and glued plates, since only boundary conditions change; (3) rib, sound post, liner strip, and end-corner block, variations are neglected; (4) all violins have a properly setup bridge and its filter effects on average are common across the conglomerated 10-violin groups; (5) flexural-extensional motion ratio changes[3] between violins are neglected; (6) plate modes 2 and 5—the lowest frequency along- and cross-grain bending modes—are primarily flexural, i.e., flat plate in character, *and* mode 5 is more important (but less flexural);[17] and (7) v_f scales simply with frequency as $v_f \propto f^{1/2}$.[21] These assumptions allow us to compute f_{crit} values for comparison with experimental values and help interpret the Dünnwald envelope high end. Knowing v_f at one frequency and applying $f^{1/2}$ scaling leads directly to estimates of f_{crit} that signal peak F_{RAD} values and initiate the high-frequency falloff. (It is an interesting "coincidence" that the bridge filter also strongly affects radiation near the F_{RAD} peak.)

2. Flexural wave velocity

Are top and back plates—doubly-curved weakly arched shells—approximately "flat"? Experimentally, (a) violin plate mode 5 (akin to the first along-grain bending mode in a flat plate) has similar portions of flexure-extension, while plate mode 2 (similar to the lowest cross-grain bending mode of a flat plate) appears close to pure flexural (nodal patterns in the inset of Fig. 7);[17] (b) a preponderance of flexural to extensional motion for top and back plates was seen in 3D mobility measurements, especially so for the maple back plates.[3] Hence we conclude that these plates are flat. The success of Schelleng's violin octet flat-plate scaling offers additional practical support for this assumption.[1,8]

The flexural wave velocity was computed directly from the lowest frequency cross- and along-grain bending modes using $v_f = f_{\#}\lambda$, where $f_{\#}$=mode 2 or 5 plate frequency. Approximate wavelengths were obtained from the maximum plate width ($L = 0.2$ m) or maximum plate length ($L = 0.35$ m), taking $\lambda \approx L$ (flat-plate value $\lambda \approx 1.33L$) for each respective direction.

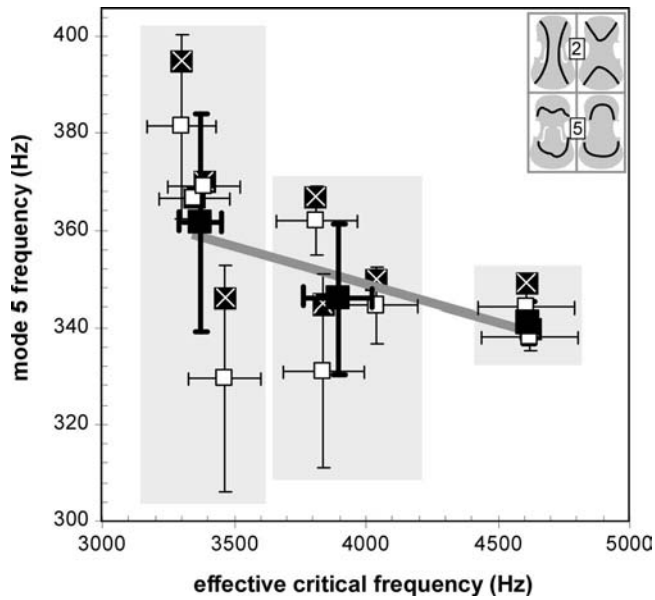

FIG. 7. Scatter plot f_{crit} vs averaged top-back (□) or maximum (⊠) mode 5 frequency for nine violins, group-averaged (■) in overlapping f_{crit} regions (grayed) with empirical trend line. S.d.'s for top-back plate frequency variations and f_{crit} estimates (horizontal). [Inset: top (with *f*-holes) and back plate mode 2 and 5 nodal patterns (note the general similarity to $B1^-$, $B1^+$ patterns in Fig. 2].

Mode 5, always clearly recognizable, has shown a wide variety of nodal line patterns ranging from irregularly arched across the upper and lower bouts—closer to pure bending?—to an almost-closed oval on the back plate that is clearly not simple bending. Such shape variations might be of some importance as well as f_5 in determining f_{crit}.

Nominal plate mode 2 and 5 frequencies of 170 and 350 Hz then lead straightforwardly to nominal flexural velocities $v_{f2} \approx 34$ m/s and $v_{f5} \approx 122$ m/s. Using the v_f scaling relationship, $f_{crit} \approx (c/v_f)^2 f_{\#} \approx (c/L)^2/f_{\#}$ the along-grain critical frequency $f_{crit} \approx (344/0.35)^2/350 \approx 2.8$ kHz, in general agreement with our effective critical frequencies for the violin, and much lower than cross-grain $f_{crit} \approx 17$ kHz, again quite similar to results for a flat plate of similar dimensions.[13] Only plate mode 5 was used in computing the critical frequencies due to much lower along-grain f_{crit}.

Based on general flexural wave properties, as plate bending mode frequency falls, f_{crit} should rise. VIOCADEAS data for nine violins with experimental plate mode and f_{crit} data (additionally grouped by averaging overlapping f_{crit} values) were plotted versus corresponding top-back plate mode 5 frequency averages in Fig. 7. The two highest f_{crit} violins had top plates tuned higher than backs, an unusual occurrence. Overall Fig. 7 indicates that f_{crit} increases as average plate mode 5 frequency decreases, although not so fast as $1/f_5$, possibly due to a "partial" flexural behavior of mode 5. Violins with wider top-back frequency spreads tended to fall further from the empirical trendline. Interestingly, the least scatter and strongest correlation for individual data points occurred when the top or back *maximum* f_5 was plotted versus f_{crit}, as can be seen in Fig. 7. Unstandardized *f*-holes and bass bar heights/shapes in the nine violins, and possibly the more variable flexural-extensional motion ratio for spruce

top plates,[3] offer likely reasons for the wider scatter among top plates.

3. f_{crit} from B1

When the plates are glued to the ribs, their modes are subsumed into the normal modes of the violin, albeit somewhere else in modal parameter space. Where substructure size-mass dominates the structure, their properties would be expected to dominate overall structural responses. As noted earlier, plate modes 2 and 5, among the lowest plate modes, emerge among the lowest corpus modes, with nodal patterns quite similar to the free-plate modes 2 and 5 (shown in the inset of Fig. 7). An empirical approximately-linear plate-$B1$ frequency correlation was revealed when the $B1$ frequency difference $\Delta B1$ and the averaged mode 5 and 2 frequency difference $\Delta 5-2$ were plotted as $\Delta B1/\Delta 5-2$ versus $\Delta B1$.[17] A heuristic dynamic "flat-plate sandwich" model indicated that $B1$ mode frequency *differences* approximately canceled rib stiffness in the overall $B1$ bending stiffness.[17]

When no plate mode frequencies are available, an empirical $B1 \rightarrow$plate mode equation can be used to estimate f_{crit}. This equation was extracted from a systematic experiment by Schleske, where plates with known mode frequencies were assembled into a strung-up violin, signature mode frequencies measured, violin top/back plate taken off, thinned incrementally, and re-glued, etc., *varing only plate thicknesses*,[26] thus eliminating many variables—different woods, shapes, archings, ribs, liners, and end-corner blocks—attending the nine violin VIOCADEAS data, which showed similar trends but with more scatter. Top and back plate trends were so similar that an empirical linear trendline was fitted through the conglomerated data for $B1^-$ and $B1^+$, resulting in the equations: $f_{B1^-}=0.233f_5+341$ Hz ($r=0.81$) and $f_{B1^+}=0.371f_5+378$ Hz ($r=0.74$). The weak dependence of $B1$ on mode 5 frequency was unsurprising, given the dominant contribution of the ribs to the overall bending stiffness.[17] This "dilution" makes working back from $B1$ frequencies to accurate plate mode frequencies much more problematic. For example, if plate mode 5 frequencies were changed by 30 Hz, the $B1$ mode frequencies would change <10 Hz ($\pm 1-2$ Hz). Where it was impossible to isolate the $B1$ modes (as in two out of three 10-violin envelopes in Fig. 6), the average $B1$ trendline equation, $f_{B1}=0.302f_5+360$ Hz, was used to estimate average plate mode 5 frequencies.

Because certain plate frequencies do not guarantee certain signature mode frequencies, such weak dependence seems to undermine the very rationale behind the traditional practice of tuning plates. However, the underlying reality is more subtle: (1) plate tuning sets f_{crit} and (2) the $A0$-$B1$ excitation mechanism proposed earlier is most strongly dependent on $B1^-$, and the frequency spread between the $B1$ modes is related to the mode 2–5 frequency spread.[17] Hence even a fairly high (average) $B1$ could have a large $\Delta B1$ and strong $\langle R_{A0}\rangle$.

A $B1$ frequency for each envelope curve in Fig. 6 was estimated by dropping down 10 dB on each side of the $B1$ envelope peak to create a band (shown superimposed on envelope) and determining its center frequency. The 10-old-Italian center frequency is shown as a dashed vertical line

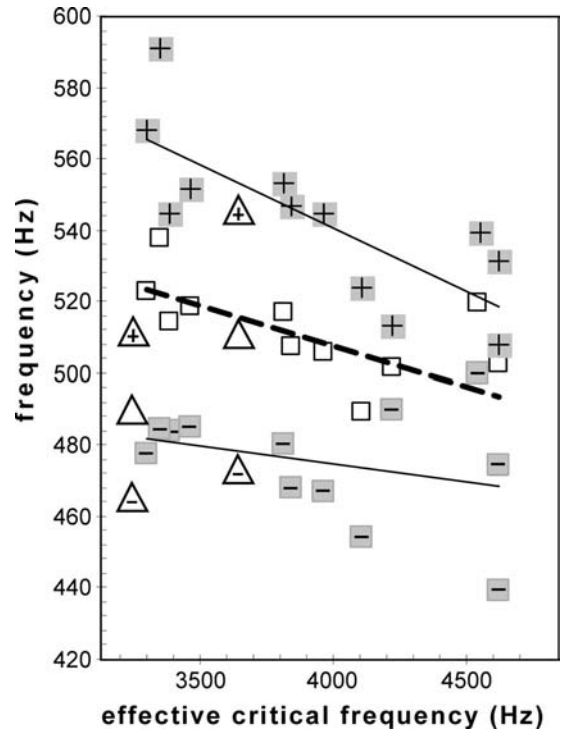

FIG. 8. First corpus bending mode frequency vs f_{crit} for 12 modern violins ($-$,+ in shaded squares for $B1^-$, $B1^+$ respectively, open squares $B1$) and 2-old Italian violins (triangles, same notation). Empirical linear trendlines for $B1^-$ (lower thin line), $B1$ (thick dashed line), and $B1^+$ (upper thin line).

across all the envelopes. Nominal graphical estimates of B1 frequency were 465, 450, and 498 Hz for the 10-old-Italian, 10-master, and 10-factory envelopes, respectively. Worthy of note is the association of lower $B1$ values in Fig. 6 with a more extended high-frequency end, and vice versa. Nominal plate mode 5 frequencies of 350 (consistent with VIOCADEAS data average), 300, and 460 Hz were computed from the $B1$ trendline, all with significant, but undeterminable, errors.

Since factory-made violins typically have plates *much* thicker than any good violinmaker would consider appropriate, such high mode 5 frequencies would not be surprising, whereas the 10-master violin set while probably low is consistent with the lack of precision in this method. In any case, such indirect rough f_{crit} calculations should be used only for examining $B1$-related f_{crit} trends. Computed f_{crit} trends, marked with arrows in Fig. 6, correspond reasonably well with the envelope frequency where radiation falls off, especially so for the 10-old-Italian and 10-factory violin subsets.

The top/back radiativity ratio (directivity)>1 indicates that the top plate radiates more effectively than the back,[3] supporting earlier measurements such as those by Meyer.[27] Modal analysis showed a plate-mode-5 shape on the top plate for $B1^+$, linked earlier to $f_{crit}\approx 3$ kHz, while the $B1^-$ top plate had a mode-2 shape, linked to ~ 17 kHz f_{crit}. On such simplistic shape-driven grounds, we conjecture that f_{crit} should show a stronger correlation with $B1^+$ than $B1^-$. The experimental test of this conjecture is presented in a scatter plot of $B1^-$, $B1^+$ (and $B1$) frequencies versus f_{crit} (Fig. 8). Overall, this shape-based conjecture is consistent with the data, especially if guided by trendline slopes. If $B1^-$, $B1^+$ frequencies are known, but separate plate mode frequencies

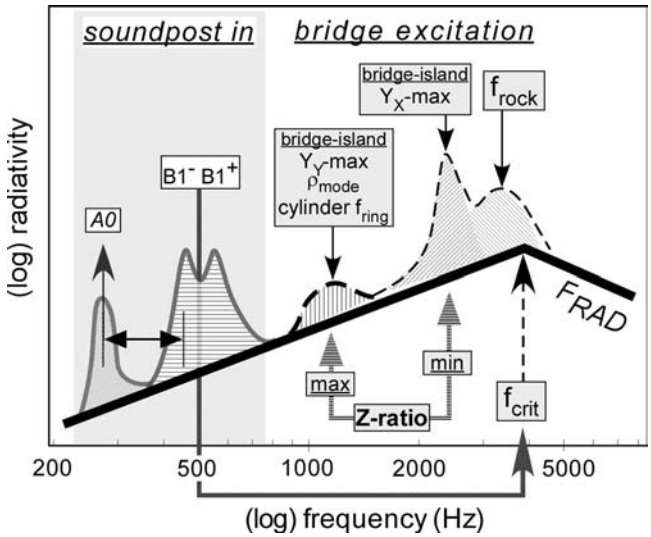

FIG. 9. Summary schema for "building" violin radiativity profile derived from this and previous work: F_{RAD} "bridgeless" violin curve ($f_{crit} \approx 3.9$ kHz, Fig. 4), $f_{ring} \approx 1$ kHz, $f_{rock} \approx 3.2$ kHz, bridge:island impedance ratio (Fig. 10, Ref. 3), soundpost (Fig. 4, Ref. 16).

are not, f_{crit} can be estimated roughly from trendlines in Fig. 8 or via our empirical $B1$-mode 5-f_{crit} equations.

We conclude with a schematic figure summarizing the various mechanisms discussed earlier that contribute to a properly setup violin's radiativity profile (Fig. 9). In our schema,

- the egress filter, F_{RAD}, underlies all radiativity profiles, with f_{crit} dependent on $B1^{(+)}$;
- the independent gatekeeper filter has a number of components—bridge-related BH and f_{rock} components at $2 < f < 4$ kHz, the nasal bump near 1.2 kHz, bridge:island impedance ratio considerations, plus sound post-linked $B1$ and its Δf excitation-dependent companion, $A0$,—superimposed on F_{RAD}.

$B1$ can now be seen to be the dominant factor at low frequencies due to its presence and $A0$-$B1$ coupling; it also sets f_{crit} at high frequencies primarily through plate mode 5. So dominating a contribution implies a significant correlation with violin sound quality judgments.

V. QUALITY JUDGMENTS

A. *B*1 and perceived quality

Martin Schleske, a leading German violin maker and leader in incorporating modal analyses into violinmaking, stated that the frequency of $B1^{(+)}$ acts as a "tonal barometer" for violin sound, with frequencies <510 Hz leading to a "somewhat 'soft' violin with dark sound lacking 'resistance'" to bowing. On the other hand, frequencies >550 Hz were characteristic of "…'stubborn' violins with bright sound, possibly with a tendency to harshness, and with strong 'resistance' to the player."[26] How do these sound quality comments relate to the radiativity profile? For instance, could a <10% change in corpus $B1^+$ frequency and any associated impedance changes cause a large change in actual—versus perceived—mechanical response? Our measurements do not support such a mechanism; surface-normal corpus impedance at the bridge feet for $B1^+$ frequencies was a local maximum almost uniformly across all violin quality classes.

There is a fascinating alternative here, a *psycho*acoustic link to the perceived playability of the violin formulated by Rohloff,[28] who noted that suppression of acoustic energy above 4 kHz caused a violinist's perception of playability to change from "easy" to "hard" speaking. Conversely, when a hard-speaking violin had frequencies >4 kHz boosted, the playability changed to easy speaking.

Viewed in the light of our radiativity profile model and these remarks (neglecting rib-related variations), if $B1^+$ gets too high it is a clear signal that the plate mode frequencies are high. This leads to a lower-than-usual f_{crit}, creating a violin with less-than-usual acoustic output above 4 kHz, while $A0$—the only resonance in the lowest octave, with a constant F_{RAD}—is also weakened if the $B1$ modes are high, removing acoustic energy from the "warm full" low-frequency band. This leaves the violin with a "compressed" profile peaked in the "bright clear" region, creating a bright sound, possibly harsh if the desired spectral balance is tilted toward the high end too much. The relative lack of acoustic energy above 4 kHz would then suggest strong resistance to the player. Conversely, $B1^+$ too low implies plate frequencies too low and f_{crit} relatively high, spreading the frequency spectrum and increasing the acoustic output above 4 kHz relative to lower frequencies, thereby suggesting a violin with less "resistance" to the player; simultaneously $A0$ is boosted tilting the spectral balance toward the low end, giving a darker sound. Thus Schleske's and Rohloff's findings actually signal a convergence in our radiativity profile model.

Acoustic characterizations of some mechanical properties have seen increasingly significant application of late. Food manufacturers now pay attention to the *acoustic* attributes of food via air and *bone conduction* transmission together in the mechanical act of chewing to improve their marketability. If the mechanical world of "hard, crispy, crackly, crunchy and snappy" is any guide,[29] a much better understanding of how acoustic signatures via air and bone conduction can color the perception of the mechanical properties of violins appears to be a productive area for future psychoacoustic research.

B. Extending qualitative

The Dünnwald 10-old-Italian subset is clear evidence that a certain type sound can be linked to certain modal attributes, the very basis of Schleske's "tonal copies" of violins.[30,31] VIOCADEAS measurements, however, showed little in the way of robust quality indicators for individual attributes—$A0$ strength being the only exception. Expanding to "coupled" parameters like the $A0$-$B1$ Δf was more productive, forcing us to closely examine the character of each signature mode. In the case of $B1$, the inherent bending character of the plates also suggested a critical frequency relationship, simultaneously linking the low and high ends of the spectrum with very few parameters.

On the other hand, qualitative evaluations suffer from too many adjectives—many of the useless sort like "nice"—

chasing too few attributes. It would be irrational to expect violins with substantially different sound, even those in the same "bad-good-excellent" general quality class, to vibrate—and thus measure—the same. Bunching them all together creates a measurement-statistical "mush" that—by itself—undermines any causal basis for a certain *single* "specification" for reliable bad-good-excellent quality classification. "Good" is no longer good enough. *Modern* violin quality rating needs a Boolean string such as "good+bright +weak-on-D-string+prominent wolf+unresponsive overall" instead of gross bad-good-excellent quality classifications to help unravel the essential modal properties linked to certain sounds and behaviors. Classifying violin quality by summing over a number of important rating criteria rather than one overall quality rating seems at this stage a much more productive way to pair violin modal and acoustic properties with sound and playability properties.

VI. CONCLUSIONS

If plate mode 5 is the underlying determiner of the violin's critical frequency—establishing radiation efficiency and damping curves, setting an F_{RAD} peak, and initiating its falloff—and if modes 2 and 5 (along with the ribs) determine the first corpus bending mode frequencies, and if the $A0$-$B1$ frequency relationship determines the strength of $A0$, then a major part of the radiativity profile is fashioned by very few parameters indeed. The ribs, woefully neglected in scientific analyses of violin sound, provide both the primary stiffness for the first corpus bending modes and the cavity so essential to violin sound at low frequencies.

Our proposed schema, rather like a Chinese puzzle that requires identification of one crucial part in order to disassemble the puzzle, provides a structural acoustics rationale for plate tap tones that buttresses their distinction as the only substructure tuned prior to assembly, even if no settled basis exists as to what the "prescribed" mode 2 and 5 frequencies should be. This hypothesized commonality of violin parametric behaviors across a wide range of quality creates a much reduced universe of things to worry about to achieve quality. This simplified model of violin radiativity provides straightforward prescriptions to achieve more desirable sound by manipulating plate and $B1$ mode frequencies. However, it always presumes the proper setup of the playable violin—sound post, bridge, and strings—so crucial to the final perception of quality.

Although a "great" violin requires the imprimatur of a great violinist, thereby greatly restricting the number of violins that can ever be labeled great, the elimination of bad violins requires only close attention to the basic details of plate tuning, general construction, and setup that have been important for centuries, aided perhaps by a few measurements of the radiativity profile for the close-to-finished violin.

[1]J. C. Schelleng, "The violin as a circuit," J. Acoust. Soc. Am. **35**, 326–338 (1963); cf. erratum, *ibid*. p. 1291.

[2]G. Weinreich, "What science knows about violins—and what it does not know," *1992 Klopsteg Memorial Lecture*, edited text published in *Research Papers in Violin Acoustics 1975–1993*, edited by C. M. Hutchins (Acoustical Society of America, Woodbury, NY, 1997).

[3]G. Bissinger, "Structural Acoustics of Good and Bad Violins," J. Acoust. Soc. Am. **124**, 1764–1773 (2008).

[4]F. A. Saunders, "The mechanical action of instruments of the violin family," J. Acoust. Soc. Am. **17**, 169–186 (1946).

[5]H. Meinel, "Regarding the sound quality of violins and a scientific basis for violin construction," J. Acoust. Soc. Am. **29**, 817–822 (1957).

[6]H. Dünnwald, "Ein erweitertes verfahren zur objectiven bestimmung der klangqualität von violinen," Acustica **71**, 269–276 (1990); modified English version "Deduction of objective quality parameters on old and new violins," J. Catgut Acoust. Soc. **1**, 1–5 (1991).

[7]G. Bissinger, "A unified materials-normal mode approach to violin acoustics," Acust. Acta Acust. **91**, 214–228 (2005).

[8]G. Bissinger, "Modal analysis of a violin octet," J. Acoust. Soc. Am. **113**, 2105–2113 (2003).

[9]G. Bissinger, "A0 and A1 coupling, arching, rib height, and f-hole geometry dependence in the 2-degree-of-freedom network model of violin cavity modes," J. Acoust. Soc. Am. **104**, 3608–3615 (1998).

[10]G. Bissinger, E. G. Williams, and N. Valdivia, "Violin *f*-hole contribution to far-field radiation via patch near-field acoustical holography," J. Acoust. Soc. Am. **121**, 3899–3906 (2007).

[11]G. Bissinger, "The violin bridge as filter," J. Acoust. Soc. Am. **120**, 482–491 (2006).

[12]F. Durup and E. Jansson, "The quest of the violin bridge-hill," Acust. Acta Acust. **91**, 206–213 (2005).

[13]L. Cremer, *The Physics of the Violin* (MIT, Cambridge, 1984).

[14]G. Bissinger, "Wall compliance and violin cavity modes," J. Acoust. Soc. Am. **113**, 1718–1723 (2003).

[15]H. Meinel, "On the frequency curves of violins," Akust. Z. **2**, 22–33 (1937).

[16]G. Bissinger, "Some mechanical and acoustical consequences of the violin soundpost," J. Acoust. Soc. Am. **97**, 3154–3164 (1995).

[17]G. Bissinger, "Surprising regularity between plate modes 2 and 5 and the B1 corpus modes: Part I," J. Violin Soc. Am.: VSA Papers, **21**, 83–101 (2007).

[18]I. P. Beldie, ""About the bridge hill mystery," J. Catgut Acoust. Soc. **4**, 9–13 (2003).

[19]J. Woodhouse, "On the bridge-hill of the violin," Acust. Acta Acust. **91**, 155–165 (2005).

[20]G. Bissinger, "Contemporary generalized normal mode violin acoustics," Acust. Acta Acust. **90**, 590–599 (2004).

[21]F. Fahy and P. Gardonio, *Sound and Structural Vibration: Radiation, Transmission and Response*, 2nd ed. (Academic, New York, 2007).

[22]G. Bissinger, "The role of radiation damping in violin sound," ARLO **5**, 82–87 (2004).

[23]M. F. Ashby *Materials Selection in Mechanical Design*, 2nd ed. (Butterworth, Heineman, 1999).

[24]K. D. Marshall, "The musician and the vibrational behavior of the violin," J. Catgut Acoust. Soc. **45**, 28–33 (1986).

[25]Ed. Heron-Allen, *Violin-Making as It Was and Is* (Ward Lock Limited, London 1885) p. 132.

[26]M. Schleske, "Empirical tools in contemporary violin making: Part 1. Analysis of design, materials, varnish and normal modes,"J. Catgut Acoust. Soc. **4**, 50–65 (2002).

[27]J. Meyer, "Directivity of the bowed string instruments and its effect on orchestral sound in concert halls," J. Acoust. Soc. Am. **51**, 1994–2009 (1972).

[28]E. Rohloff, "The speaking of violin sounds," Z. Angew. Phys. **17**, 62–63 (1964). English abstract published in *Musical Acoustics, Part II, Violin Family Functions*, Benchmark Papers in Acoustics Vol. **6**, edited by C. M. Hutchins (Dowden, Hutchinson & Ross, Stroudsburg, PA, 1976).

[29]B. Reynaud *et al.*, "Acoustic signature of hard, crispy, crackly, crunchy and snappy," Proceedings of the 19th International Congress on Acoustics, Madrid 2007, paper No. ppa-02-022.

[30]M. Schleske, "On making 'tonal copies' of a violin," J. Catgut Acoust. Soc. **3**, 18–28 (1996).

[31]M. Schleske, webpage, http://www.schleske.de/11handbuch/en_extras3handbuch04klangfarbe.pdf (Last viewed July 2008).